Supporting Information

Protein sequencies for MaDA-1 and MaDA-3

Protein sequence for MaDA-1: THEAFLECLTTRIPSNSTFTPQSIIYTPDNPSYSTIL
DSTTQNPRFLSSSTRNPFAIITPLHASHIQAALYCSQKHGEQMRIRSGGDYEGLSYQS
SVPFFILDLRNLSSISIDAKSKSAWVQAGATIGELYYGIAKTSLNLSFPGGVAHTIGVG
GQLGGGGYGYSTRKYGLASDNVIDAQLIDARGRILDRKTMGEDLFWAIRGGGAGSF
GIVLAWKIRLVNTPSTVTIFEAVRSWENNTTKKFIRRYQRRASKTDKDLTIFVGFRT
TSSTDEEGNERISILTIVSATFHGSKDRLLQLVQKEFPDLGLVSEECTEMSWVRSIIHF
NLFGDEVPLEVLLNRTLNFEMKAFKLRSDYVQKPIPDDVLEKLLSKLYDEETGXGYI
EFFPYGGKMSKISESEIPFPYRAGNLYNLRYMVSWKDDGNITRTNMHLSWIKDAYD
YMTPYVSKDPRGAYLNFRDLDIGVNVNESDYDYVAKASVWGTKYFRNNFYRLVDI
KTIVDPTNFFKYEQSIPPLPPL

Protein sequence for MaDA-3: HESFLECLTTRISKSNSTSTPESIIYTKDNPSYSTILN
STSLNPRFFPSSARYPLLIVTPLHASHVQATVHCAKKHGIQIRIRSGGDYEGLSYMSN
VTFAIVDLRNLSSIDVDVKRKSAWVQSGATLGELHYWIAKKSQNLAFPGVVGHTVG
IGGMLGAGGYGYSSRKYGLSADNILDAQLIDVRGRILNRKSMGEDLFWAIRGGGAG
SFGIVLAWKVRLVDVPSKVTVFTAIRDWDNNATKKFIHRYQRRIAKVDKDLTIIVRF
LTASITDEKGSKKIQISTFITATYHGSQDRLLSLMEKEFPELGLLAKECAEGAWVQSI
LYFNLLTNSKSLDVLLNRTLNFEWRAFKIKSDYLKKPIPDQVLENLLVKLYEEDIGET
FVEFFPYGGKLDEISESEIPCPHRAGNLYNLRYMVLWKEGQNATAVNKHLSWIRRA
YNYMTPYVSKNPRGAFLNFRDLDIGTNPNENEINGAYNYIKQASNWGTKYFKNNF
YKLIYVKTIVDPTNFFTYEQSIPSLLPH

For clarity, all MaDA-1 residues were aligned to the numbering scheme where the corresponding site is labeled as position 294 (originally 283 in the native sequence).

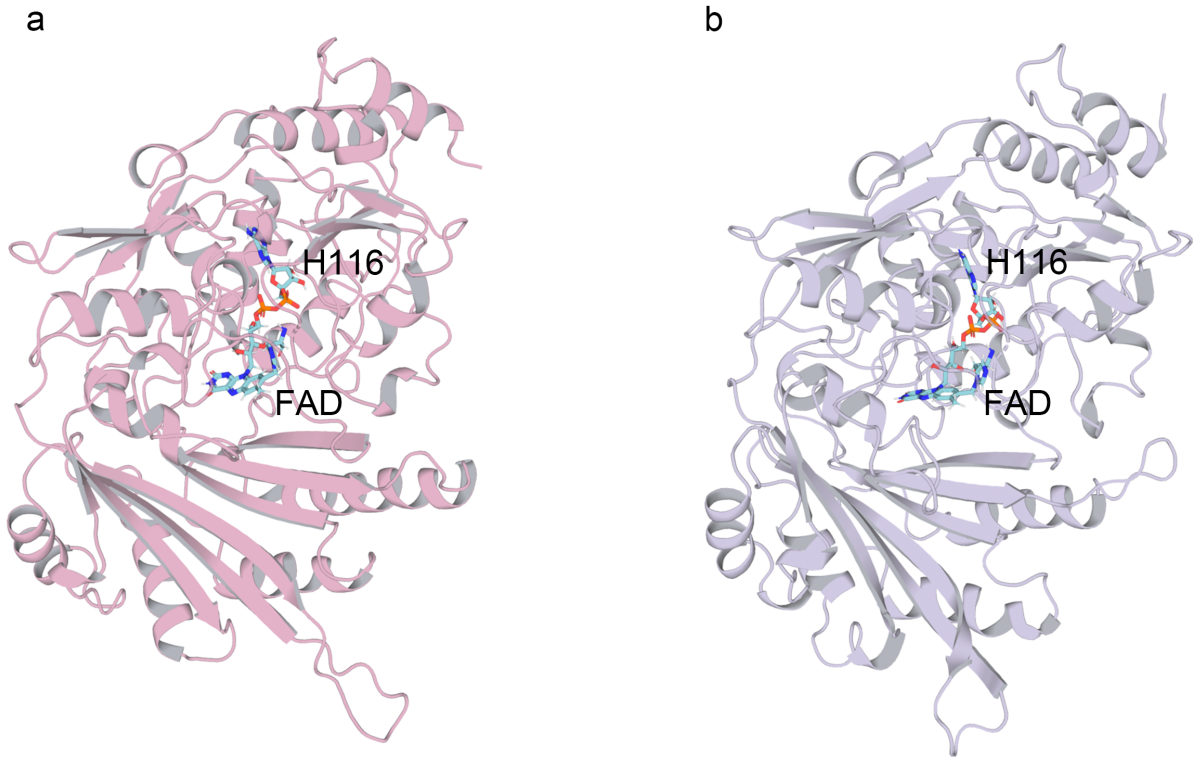

Figure S1: Overall structures of (**a**) MaDA-1 and (**b**) MaDA-3 showing the covalent linkage between residue H116 and the flavin adenine dinucleotide (FAD).

Table S1: Parameters of histidine-covalently bound flavin adenine dinucleotide (FAD).

No.	Atom	Type	M/E	i	j	k	Bond	Angle	Dihedral	Charge
1	DUMM	DU	M	0	-1	-2	0.0000	0.000	0.000	0.000000
2	DUMM	DU	M	1	0	-1	1.4490	0.000	0.000	0.000000
3	DUMM	DU	M	2	1	0	1.5230	111.210	0.000	0.000000
4	N1	N	M	3	2	1	1.5400	111.208	-180.000	-0.417500
5	H1	H	E	4	3	2	1.0300	92.003	-119.703	0.271900
6	C1	CT	M	4	3	2	1.4510	60.971	117.717	5.174981
7	C3	CT	3	6	4	3	1.5300	111.207	49.539	-3.117144
8	C4	cc	S	7	6	4	1.4940	114.632	-65.986	0.226420
9	C5	cd	B	8	7	6	1.3710	130.549	68.868	-0.232670
10	N3	nd	S	9	8	7	1.3750	111.078	-178.411	-0.472672
11	C6	cc	B	10	9	8	1.3130	104.791	-0.412	-0.022172
12	N2	na	S	11	10	9	1.3610	112.513	0.503	0.378016
13	C30	c3	3	12	11	10	1.4590	124.733	-172.992	-0.041819
14	C28	ca	S	13	12	11	1.5220	112.134	83.147	0.077281
15	C26	ca	B	14	13	12	1.4190	121.258	-102.237	0.157018
16	C24	ca	B	15	14	13	1.3800	117.909	176.983	-0.372100
17	C23	ca	S	16	15	14	1.4060	122.005	-0.003	0.467513
18	N9	nc	S	17	16	15	1.3680	118.574	-178.827	-0.542606
19	C20	cd	S	18	17	16	1.2930	117.889	177.624	0.198957
20	C17	c	B	19	18	17	1.4940	118.340	-179.125	0.732680
21	N7	ns	B	20	19	18	1.3720	112.908	177.839	-0.800473
22	C13	c	B	21	20	19	1.4070	127.287	-1.314	0.986180
23	N5	nc	S	22	21	20	1.3730	118.404	2.691	-0.762119
24	C33	cd	S	23	22	21	1.3140	119.513	-0.642	0.467667

No.	Atom	Type	M/E	i	j	k	Bond	Angle	Dihedral	Charge
25	N13	na	B	24	23	22	1.3620	119.084	176.897	-0.119372
26	C11	c3	3	25	24	23	1.4700	118.275	-6.469	0.534845
27	C10	c3	3	26	25	24	1.5360	112.140	90.744	-0.207242
28	C9	c3	3	27	26	25	1.5430	109.564	-170.369	0.561695
29	C8	c3	3	28	27	26	1.5400	112.478	-178.743	0.403112
30	C7	c3	3	29	28	27	1.5180	112.734	64.954	-1.558148
31	O6	os	S	30	29	28	1.4210	108.230	-179.729	-0.474605
32	P1	p5	3	31	30	29	1.6410	116.341	-171.104	1.412955
33	O3	o	E	32	31	30	1.4890	107.533	-166.866	-0.808147
34	O4	o	E	32	31	30	1.5100	108.774	-33.769	-0.808147
35	O5	os	S	32	31	30	1.6460	101.215	75.044	0.044056
36	P2	p5	3	35	32	31	1.6380	132.113	55.795	0.507009
37	O10	o	E	36	35	32	1.5070	103.921	171.129	-0.639459
38	O12	o	E	36	35	32	1.4890	112.685	36.923	-0.639459
39	O17	os	S	36	35	32	1.6590	101.422	-75.770	-0.084483
40	C22	c3	3	39	36	35	1.4270	118.991	-82.142	0.328170
41	C19	c5	B	40	39	36	1.5120	112.285	-100.140	0.423189
42	C16	c5	3	41	40	39	1.5300	115.990	46.147	-0.129213
43	C15	c5	3	42	41	40	1.5230	100.964	-160.062	0.234821
44	C12	c5	3	43	42	41	1.5370	100.452	39.273	0.414520
45	O16	os	E	44	43	42	1.4040	107.244	-28.501	-0.649321
46	N12	na	S	44	43	42	1.4600	111.855	90.101	-0.189541
47	C18	ca	S	46	44	43	1.3720	126.074	88.025	0.432342
48	N8	nb	S	47	46	44	1.3400	128.013	1.324	-0.806597
49	C14	ca	B	48	47	46	1.3300	111.175	-179.909	0.656319
50	N6	nb	S	49	48	47	1.3400	128.869	0.074	-0.870681

No.	Atom	Type	M/E	i	j	k	Bond	Angle	Dihedral	Charge
51	C25	ca	B	50	49	48	1.3440	118.496	-0.179	0.816410
52	C21	ca	S	51	50	49	1.4090	118.580	0.191	-0.060951
53	N11	nc	S	52	51	50	1.3820	132.830	179.581	-0.605209
54	C29	cd	S	53	52	51	1.3100	103.881	-179.723	0.357833
55	H32	h5	E	54	53	52	1.0830	125.595	179.979	0.069179
56	N10	nv	B	51	50	49	1.3500	119.001	-178.320	-0.959567
57	H30	hn	E	56	51	50	1.0090	118.146	-13.341	0.408850
58	H31	hn	E	56	51	50	1.0080	119.131	-167.242	0.408850
59	H20	h5	E	49	48	47	1.0870	115.951	179.995	0.025367
60	H17	h2	E	44	43	42	1.0940	111.159	-149.987	0.104768
61	O13	oh	S	43	42	41	1.4100	110.872	-75.233	-0.739636
62	H22	ho	E	61	43	42	0.9690	106.031	-39.825	0.453073
63	H21	h1	E	43	42	41	1.0970	113.501	158.400	0.053807
64	O14	oh	S	42	41	40	1.3970	113.866	78.788	-0.631222
65	H26	ho	E	64	42	41	0.9860	103.383	-81.638	0.486135
66	H25	h1	E	42	41	40	1.0970	109.410	-46.148	0.051441
67	H27	h1	E	41	40	39	1.0970	108.046	168.489	-0.019227
68	H28	h1	E	40	39	36	1.0910	107.572	139.361	-0.136905
69	H29	h1	E	40	39	36	1.0920	110.138	21.084	-0.136905
70	H23	h1	E	30	29	28	1.0990	110.419	59.799	0.652145
71	H24	h1	E	30	29	28	1.0950	110.532	-60.311	0.652145
72	O7	oh	S	29	28	27	1.4130	108.518	-170.811	-0.704144
73	H19	ho	E	72	29	28	0.9720	108.416	-134.254	0.549111
74	H18	h1	E	29	28	27	1.0980	106.730	-53.018	-0.050955
75	O8	oh	S	28	27	26	1.4100	111.703	-48.405	-0.688436
76	H16	ho	E	75	28	27	0.9760	113.050	-67.208	0.634368

No.	Atom	Type	M/E	i	j	k	Bond	Angle	Dihedral	Charge
77	H15	h1	E	28	27	26	1.0980	106.761	65.663	0.020906
78	O9	oh	S	27	26	25	1.4100	111.852	-46.389	-0.632103
79	H14	ho	E	78	27	26	0.9730	107.478	-40.831	0.434002
80	H13	h1	E	27	26	25	1.0980	108.476	69.520	0.274207
81	H11	h1	E	26	25	24	1.0900	106.608	-29.834	-0.187717
82	H12	h1	E	26	25	24	1.0890	108.889	-145.610	-0.187717
83	C32	ca	S	25	24	23	1.3870	120.445	172.596	0.033746
84	C31	ca	S	83	25	24	1.4000	122.857	-173.474	-0.552176
85	H10	ha	E	84	83	25	1.0800	119.841	0.640	0.637770
86	O11	o	E	22	21	20	1.2180	118.716	-177.326	-0.637918
87	H8	hn	E	21	20	19	1.0130	117.000	-179.338	0.397886
88	O15	o	E	20	19	18	1.2150	124.012	-2.076	-0.588912
89	H9	ha	E	16	15	14	1.0850	120.914	-179.581	0.213440
90	C27	c3	3	15	14	13	1.5080	122.273	-3.434	-0.387976
91	H33	hc	E	90	15	14	1.0920	110.371	-177.955	0.116842
92	H34	hc	E	90	15	14	1.0950	111.825	62.488	0.116842
93	H35	hc	E	90	15	14	1.0940	111.680	-58.177	0.116842
94	H36	h1	E	13	12	11	1.0900	107.572	-39.463	0.048601
95	H37	h1	E	13	12	11	1.0910	108.659	-154.520	0.048601
96	H6	h5	E	11	10	9	1.0810	125.741	179.756	0.121567
97	H5	h4	E	9	8	7	1.0830	126.484	2.002	0.344943
98	H3	hc	E	7	6	4	1.0920	108.602	56.520	0.005100
99	H4	hc	E	7	6	4	1.0900	106.494	170.251	0.005100
100	H2	H1	E	6	4	3	1.0960	107.839	-70.728	-1.107557
101	C2	C	M	6	4	3	1.5430	110.836	171.541	0.597300
102	O2	O	E	101	6	4	1.2360	122.064	-113.217	-0.567900

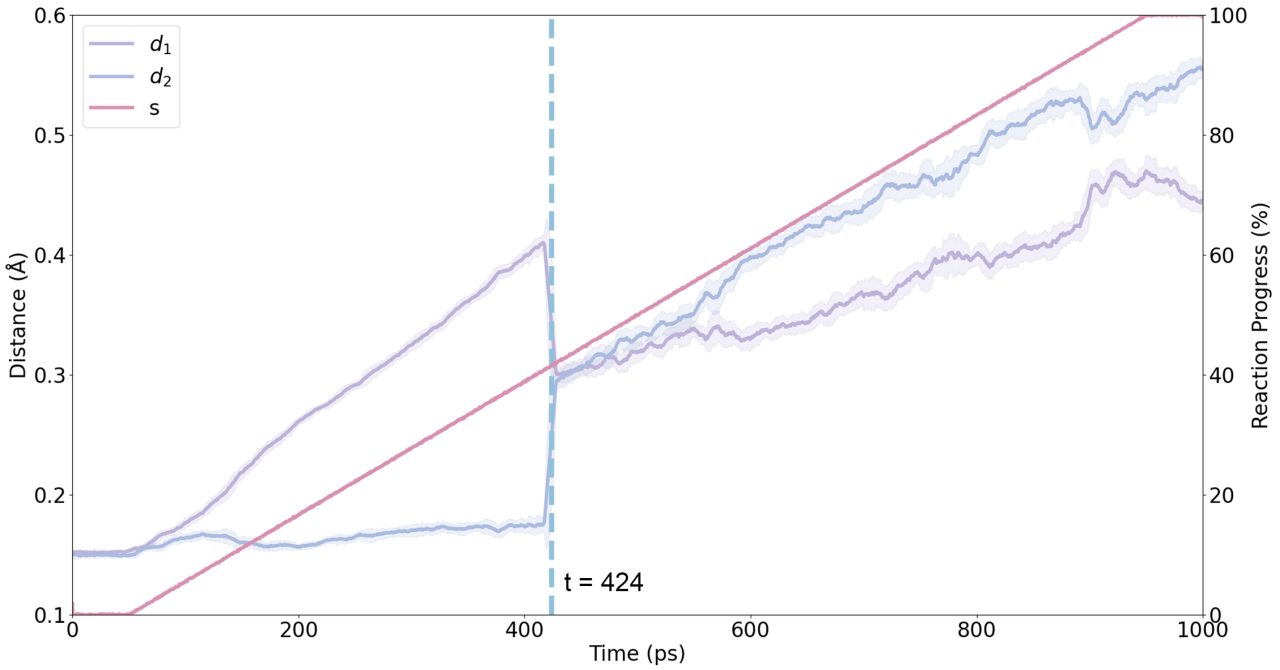

Figure S2: Steered MD validation of CV suitability. d_1 and d_2 correspond to the two forming C–C bonds, while the path-CV coordinate s denotes the progress along the reaction pathway.

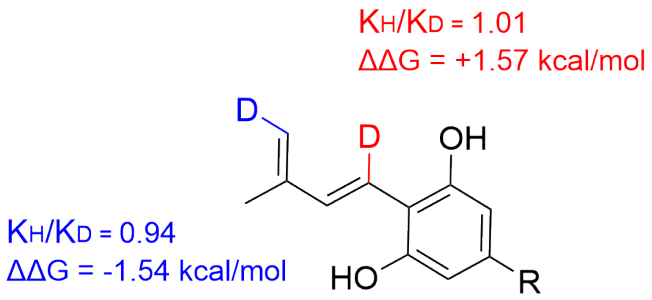

Figure S3: Kinetic isotope effects from experiment and computation. Deuterium substitution was introduced at the two carbon atoms involved in the Diels–Alder reaction. The experimental KIE was characterized by the $K_{\mathrm{H}}/K_{\mathrm{D}}$ ratio, whereas the computational $\Delta\Delta G$ values were obtained from ML/MM MetaD simulations as $\Delta G_{\mathrm{D}} - \Delta G_{\mathrm{H}}$.

Table S2: Activation free energies ($\Delta G^{\ddagger}$, kcal mol^{-1}) of MaDA1 and MaDA3 along the *endo*/*exo* pathways, as obtained from experiment, DFT cluster models, and ML/MM metadynamics. The symbol / denotes cases where no previous experimental or computational data were available. All energies are reported in kcal mol^{-1}.

	MaDA3 *endo*	MaDA3 *exo*	MaDA1 *endo*	MaDA1 *exo*	Aqueous *endo*	Aqueous *exo*
Experimental	/	19.29	16.14	/	/	/
DFT cluster	/	20.8	20.3	/	23.3	26.1
ML/MM MetaD	30.04	25.75	25.08	29.33	27.68	30.31

Table S3: Endo/Exo selectivity ratios and activation free energies ($\Delta G^{\ddagger}$, $\mathrm{kcal\,mol^{-1}}$) of MaDA3 variants from experiment and ML/MM metadynamics simulations. The ratio refers to the relative endo:exo product distribution. $\Delta\Delta G = \Delta G_{\mathrm{endo}} - \Delta G_{\mathrm{exo}}$, with positive values favoring the *exo* pathway.

	MaDA3-R294G	MaDA3-R294A	MaDA3-Mu3	MaDA3-Mu5
Experimental ratio (endo:exo)	1:3.8	1:1.2	1:1	1:0.5
Computational ratio (endo:exo)	1:10.6	1:1.38	1:6.4	1:1.36
ΔG_{endo} ($\mathrm{kcal\,mol^{-1}}$)	27.27	26.88	26.69	27.50
ΔG_{exo} ($\mathrm{kcal\,mol^{-1}}$)	25.87	26.69	27.88	27.30
Experimental $\Delta\Delta G$ ($\mathrm{kcal\,mol^{-1}}$)	0.86	0.11	0	−0.45
Computational $\Delta\Delta G$ ($\mathrm{kcal\,mol^{-1}}$)	1.40	0.19	1.19	0.20

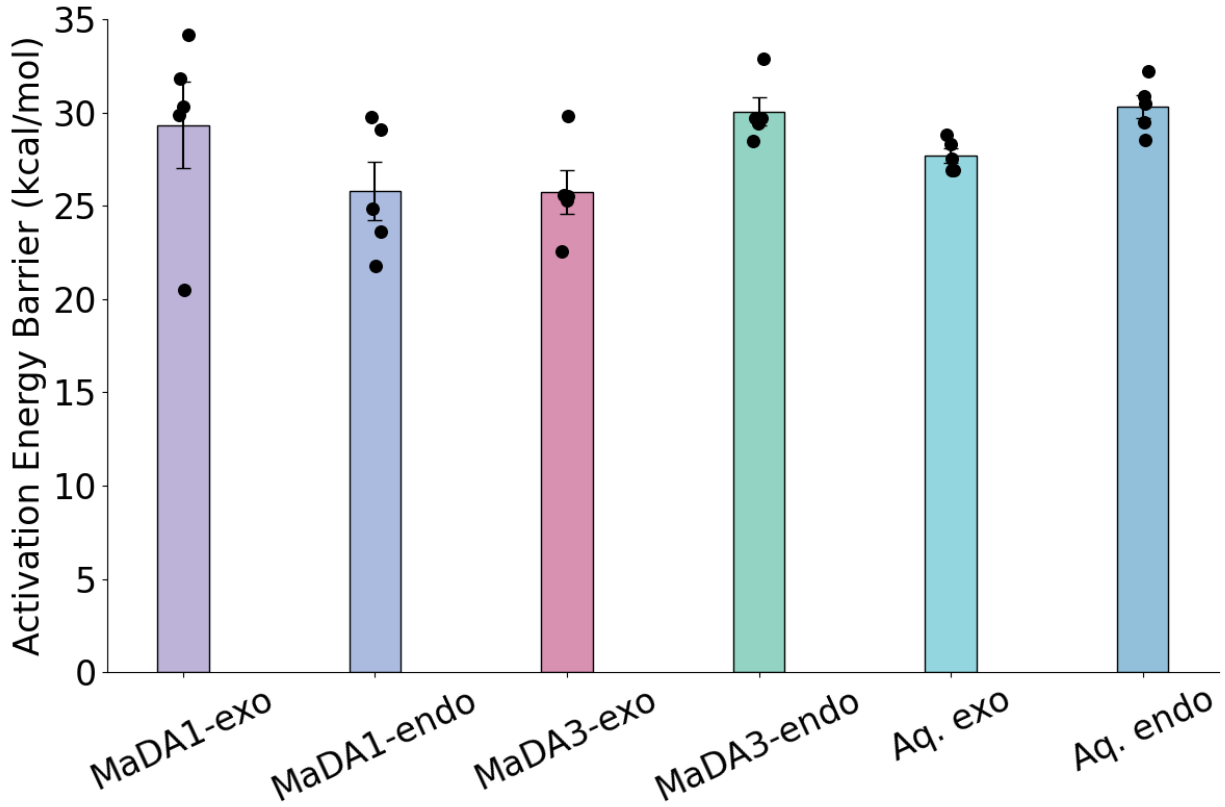

Figure S4: Activation energy barriers for Diels–Alder reactions in three environments (MaDA1, MaDA3, and aqueous solution) for two enantiomers. Each bar represents the mean barrier height, with error bars indicating the standard error of the mean. Individual black dots denote raw data points.

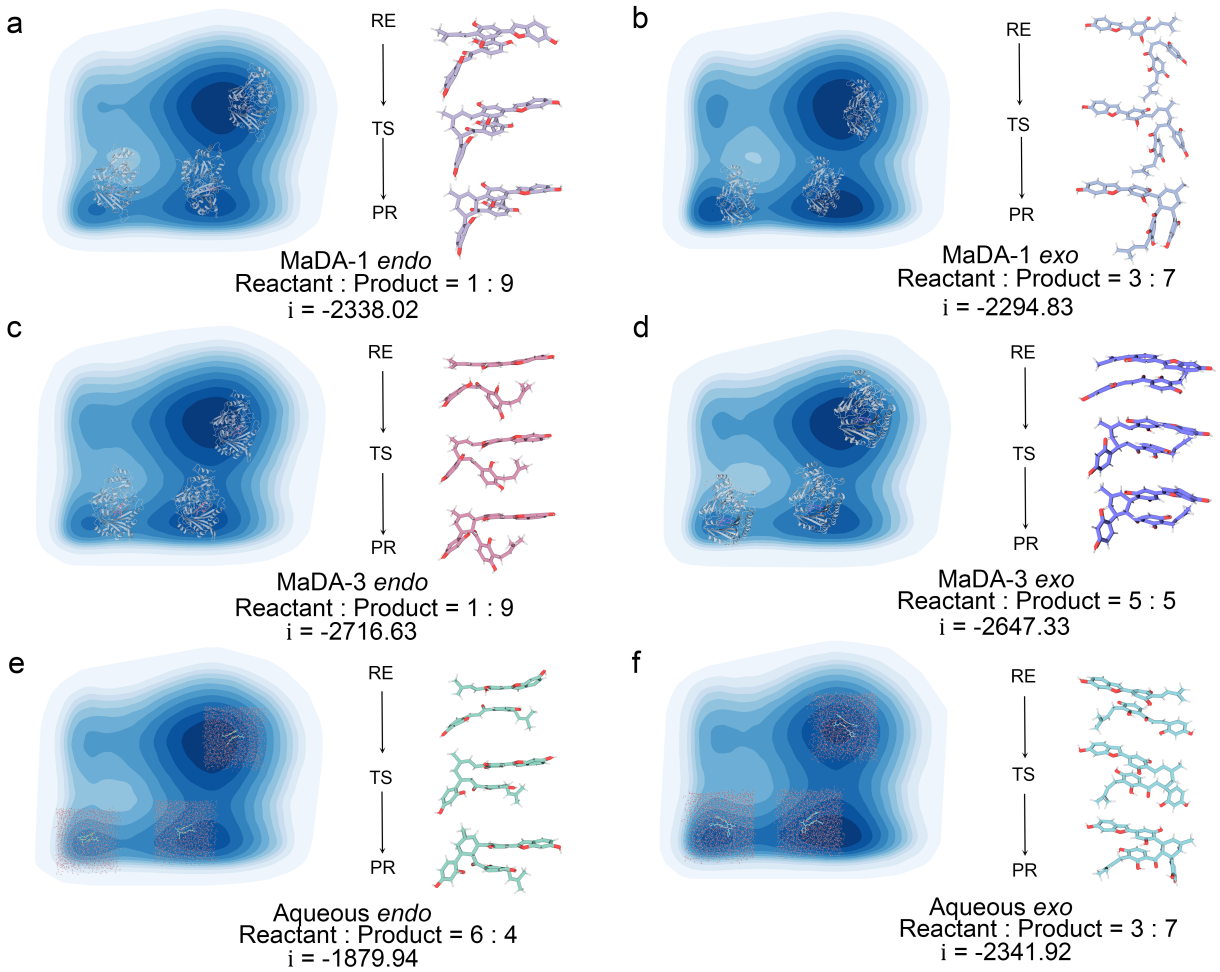

Figure S5: Committor and frequency analysis of putative TS structures. Potential TS structures and the corresponding reactant and product states identified by committor analysis are shown for MaDA-1, MaDA-3, and aqueous conditions, for both *exo* and *endo* enantiomers. For each candidate TS, ten independent trajectories were propagated, and the numbers reaching reactant or product basins are reported. The imaginary frequencies of the validated TS structures were calculated and are reported in cm^{-1}.

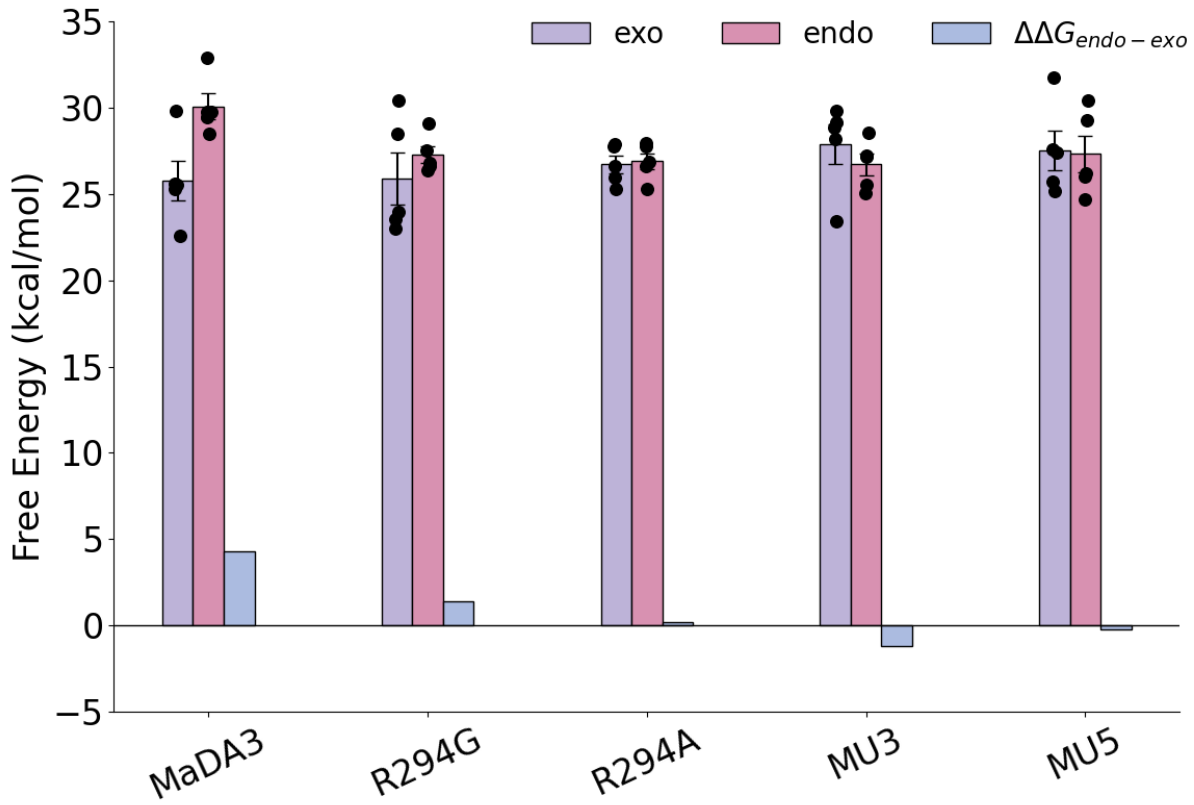

Figure S6: Comparison of free energy barriers for Diels–Alder reactions across different enzyme variants (MaDA3, R294G, R294A, MU3, and MU5). Bars represent mean activation free energies for the exo (purple) and endo (pink) pathways, with error bars indicating the standard error of the mean. Black dots correspond to individual data points. The blue bars denote the relative enantiomeric selectivity, expressed as $\Delta G_{endo} - \Delta G_{exo}$.